Journal of Power Sources 196 (2011) 301–312

Contents lists available at ScienceDirect

Journal of Power Sources

journal homepage: www.elsevier.com/locate/jpowsour

Experimental analysis of performance degradation of micro-tubular solid oxide fuel cells fed by different fuel mixtures

F. Calise [a], G. Restucccia [a,*], N. Sammes [b]

[a] DETEC - University of Naples Federico II, P.le Tecchio 80, 80125 Naples, Italy
[b] Department of Metallurgical and Materials Engineering, Colorado School of Mines, 1500 Illinois Street, Golden, CO 80401, USA

ARTICLE INFO

Article history:
Received 1 March 2010
Received in revised form 19 April 2010
Accepted 2 June 2010
Available online 10 June 2010

Keywords:
SOFC
Micro-tubular
Carbon deposition
Degradation
Fuel mixtures

ABSTRACT

This paper analyzes the thermodynamic and electrochemical dynamic performance of an anode supported micro-tubular solid oxide fuel cell (SOFC) fed by different types of fuel. The micro-tubular SOFC used is anode supported, consisting of a NiO and $Gd_{0.2}Ce_{0.8}O_{2-x}$ (GDC) cermet anode, thin GDC electrolyte, and a $La_{0.6}Sr_{0.4}Co_{0.2}Fe_{0.8}O_{3-y}$ (LSCF) and GDC cermet cathode. The fabrication of the cells under investigation is briefly summarized, with emphasis on the innovations with respect to traditional techniques. Such micro-tubular cells were tested using a Test Stand consisting of: a vertical tubular furnace, an electrical load, a galvanostast, a bubbler, gas pipelines, temperature, pressure and flow meters. The tests on the micro-SOFC were performed using H_2, CO, CH_4 and H_2O in different combinations at 550 °C, to determine the cell polarization curves under several load cycles. Long-term experimental tests were also performed in order to assess degradation of the electrochemical performance of the cell. Results of the tests were analyzed aiming at determining the sources of the cell performance degradation. Authors concluded that the cell under investigation is particularly sensitive to the carbon deposition which significantly reduces cell performance, after few cycles, when fed by light hydrocarbons. A significant performance degradation is also detected when hydrogen is used as fuel. In this case, the authors ascribe the degradation to the micro-cracks, the change in materials crystalline structure and problems with electrical connections.

1. Introduction

Fuel cells are well known electrochemical devices capable to convert directly the chemical energy of the fuel in electricity and heat. The operating principle of this device is well known since 1800 but a substantial industrial and academic research effort has been performed only in the last few years. This recent renaissance in fuel cell research is due to the combination of the dramatic decrease of fossil fuels availability and to the fuel cell peculiarities, such as: high electrical and thermal efficiencies and low emissions [1]. Among fuel cell technologies, the solid oxide fuel cells (SOFCs) are considered one of the most promising technologies for distributed power/heat production, due to: large availability of high temperature heat for cogeneration purposes, capability to be fed by hydrocarbons and good reliability [2,3].

In particular, SOFCs are very promising for their capability to direct internally convert methane into hydrogen, available for the electrochemical reactions [4]. This arrangement is very profitable since dramatically simplifies system layout, also decreasing system capital cost. Literature is very rich of theoretical [5,6] and experimental [7,8] studies of direct internal reforming SOFCs, as discussed in the following section [9].

Presently, a number of different SOFC configurations are under investigation, namely: tubular, planar, tubular high power density (HPD) and micro-tubular [3,10]. Nevertheless, SOFCs are still far from commercial availability, mainly due to problems such as: cost targets, operating life and reliability [10].

Solid oxide fuel cell applications have long been limited by the necessity to operate at high temperatures, causing prolonged start up times and materials constraints, among other cost increasing constraints [2,3,10]. Considerably decreasing the operating temperature of SOFCs is necessary for efficient power production, specifically in mobile applications where start up time and materials cost is of increasing importance. Reducing the operating temperature of SOFCs below 650 °C can extend the lifetime of the SOFC stack, lower cost by allowing the use of metal materials, and can decrease the degradation of SOFC and stack materials [11,12]. Tubular SOFC designs have been shown to be stable for repeated cycling under rapid changes in electrical load and in cell operating temperatures [13–15]. However, tubular SOFC capital costs are very high end significantly far from the target of 400 US$ kW^{-1}, planned by SECA. This is mainly due to their low power density and

* Corresponding author. Tel.: +39 0817682299; fax: +39 0812390364.
E-mail address: giulio.restuccia@unina.it (G. Restucccia).

0378-7753/$ – see front matter © 2010 Elsevier B.V. All rights reserved.
doi:10.1016/j.jpowsour.2010.06.010

to the materials to be used for a safe operation at the high temperatures typical of SOFC stacks. In this framework, micro-tubular SOFCs aim at solving the problems affecting the typical tubular SOFC. In fact, their lower diameter and operating temperature promise to: (i) reduce capital costs; (ii) increase power density; (iii) increase thermal shock resistance; and (iv) reducing start up and shut down times. In fact, micro-tubular SOFCs have also been shown to be able to endure the thermal stresses associated with rapid heating up to operating temperatures [16,17]. In contrast to planar SOFC designs, when the diameter of the tubular SOFC is decreased, it is possible to design SOFC stacks for high volumetric power densities [2,18].

The first micro-tubular stack prototype was pioneered by the group of Kendall in the early 1990s. Then, their development was prevalently due to the work of the research groups of Prof. Kendall and Prof. Sammes [19]. However, innovative micro-tubular stack designs are very rare. In fact, the research is still focused in the attempt to eliminate the problems of the single cells and consequently the stack design becomes a secondary issue.

In fact, several problems of micro-tubular SOFCs are still to be solved for a safe and reliable operation, in systems such as vehicles or on small-sized cogenerative power plants. Therefore, such cells should be subject to continuous start up and shut down which still determine a significant performance degradation. In fact, the anode of these cells usually consists of coarse and fine YSZ particles (used to comply with electrolyte thermal expansion coefficient and to prevent Ni particles from agglomeration and sintering) with NiO nanoparticles [1]. Here, assuming no purge gas is used, Ni particles are continuously reduced and oxidized respectively during the start up and shut-down of the cell. This redox cycling determines a mechanical stress in the cell, caused by expansion and shrinkage, which can seriously damage anode structure, causing cracks and delamination. In addition, this cycling also induces fatigue and thermal stresses in the cell structure, also increasing the residual stresses due the fabrication process [1]. All these phenomena may determine a significant electrochemical performance degradation or an eventual failure.

Also, micro-tubular SOFCs are particularly sensitive to carbon deposition, as explained in detail in the next section. Therefore, when fed by CO or hydrocarbons the cell may fail after few hours of operation.

Literature data dealing with thermal, electrical and electrochemical performance of micro-tubular SOFCs are scarce, particularly regarding to electrochemical performance degradation due to redox and thermal cycling and to carbon deposition. Only a few studies on this topic are found in literature, mainly due to the groups of Kendall and Sammes. In particular, the electrochemical performance of a Ni/YSZ/LSM micro-tubular cell fed by methane was investigated in [20]. In this paper, the authors used methane both as reductant and fuel and performed a parametric analysis in order to detect the optimal reduction time. They also concluded that carbon deposition occurs at high methane flow rates when the methane partial oxidation is not sufficiently fast to reform all the methane flowing in the cell. Another experimental study [1] by the same research group investigated the effects of redox cycling on the anode of a NI-YSZ micro-tubular cell. Using SEM micrographs, authors assessed that the main sources of the electrochemical degradation were micro-crack formation in the anode and delamination at the electrolyte-electrode interface. A study on the same topic was also performed in [21], where the effects of redox cycling on a Ni/8YSZ supported SOFC were investigated, concluding that the appropriate selection of particle size is mandatory in order to achieve good mechanical and electrochemical stability. The same type of micro-tubular cell was also optimized in [22] for a direct use with methane in order to avoid the effects of carbon deposition.

Table 1
ΔG° at 298 K and at 1123 K and the equilibrium temperature for the major reactions of a SOFC powered by methane.

Reaction	ΔG° (298 K) (kJ mol^{-1})	$T_{\Delta G=0}$ (K)	ΔG° (1123 K) (kJ mol^{-1})
1. $CH_4 + 2O_2 = CO_2 + 2H_2O$	−800.9	154.3	−796.5
2. $CH_4 + ½O_2 = CO + 2H_2$	−86.5	210	−277
3. $H_2 + ½O_2 = H_2O$	−228.6	5.4	−179
4. $CO + ½O_2 = CO_2$	−257.2	3.3	−186
5. $CH_4 + CO_2 = 2CO + 2H_2$	+170.7	963	−41
6. $CH_4 + H_2O = CO + 3H_2$	+142.1	960	−35
7. $CO + H_2O = CO_2 + H_2$	−55.3	955	+6
8. $CH_4 = C + 2H_2$	+50.7	926	−16
9. $CO + H_2 = C + H_2O$	−91.4	981	+19
10. $2CO = C + CO_2$	−120.5	980	+25

Most of the cited papers dealt with Ni/ YSZ cells and are basically focused on hydrogen as fuel. However, it is also well known that carbon deposition can be mitigated using dopants such as ceria and molybdenum in the anode. Therefore, in this paper an anode supported micro-tubular SOFCs with a cermet anode of NiO and GDC (Gadolinum Doped Ceria), a GDC electrolyte and a cathode in LSCF ($La_{0.6}Sr_{0.4}Co_{0.2}Fe_{0.8}O_{3-y}$), was considered. A preliminary study was recently published by the authors [23] showing the electrochemical performance of this kind of cell, fed by H_2, at different values of operating temperature and fuel flow rate. In this paper, authors show the results of an experimental analysis in which the same cells were tested at the operating temperature of 550 °C, using different combinations of CO, H_2O, CH_4 and H_2 as fuels. Such experimental analysis was carried out varying fuel composition under many load cycles, in order to assess the corresponding effects on the cell electrochemical performance degradation.

2. Theory

This section briefly summarize the major chemical reactions occurring on the anode surface of a solid oxide fuel cells when is fed with light hydrocarbon fuels, as methane, paying special attention to the carbon deposition phenomena.

2.1. Governing reactions: oxidation and carbon deposition

Although the operating principle of a fuel cell fed by hydrogen is simple, the operation by methane is much more complicated and leads to a series of at least 10 major reactions. A summary of these reactions is given in Table 1. These reactions can be conveniently split into four groups, although there is some overlap between them.

1. The oxidation steps: these are reactions 1–4 in Table 1. These reactions are the only responsible for current production within a SOFC as the electrons are carried through the cell by O^{2-}, completing the circuit. These reactions are all favorable at SOFCs operating temperature (650–1250 K). Previous works suggested that the direct oxidation of methane (reactions 1 and 2) does not usually contribute to the power production of the cell leaving steps 3 and 4 as the power producing reactions [4]. Thus, reactions which produce hydrogen and carbon monoxide will indirectly contribute to the cell electrical power production and efficiency.
2. Steam methane reforming (SMR) reactions: reactions 2, 5 and 6, which can convert methane into the more useful hydrogen and carbon monoxide.
3. Water gas shift (WGS) reaction 7, which converts CO and water into hydrogen and carbon dioxide.
4. Carbon forming reactions: as a byproduct of reactions 8–10, carbon is formed, which, if severe enough, can block the small

diameter tubes causing the system to fail. Reactions 9 and 10 become thermodynamically less favorable as the temperature increases and become more unfavorable above 981 K. Unfortunately, reaction 8 becomes more favorable with increasing temperature and is thermodynamically favorable above 926 K. Thus, temperature control alone cannot prevent the deposition of carbon. As one of the reaction products is solid (i.e. carbon, which is effectively removed from the reaction mixture), pulling the equilibrium over to the right, carbon formation can take place. Carbon formation may be reduced as suggested by Table 1 (data taken from Ref. [24]), i.e.: increasing carbon dioxide partial pressure or promoting the water gas shift reaction (which has the bonus of removing carbon monoxide from reaction 9 and producing carbon dioxide, pushing reaction 10 to the left).

Previous works suggested that SOFCs are better able to utilize hydrogen as a fuel source, rather than carbon monoxide [9]. In fact, H_2 kinetics is faster and CO may determine significant problems due the eventual carbon deposition [4]. Reaction 7 becomes thermodynamically unfavorable above 955 K which is below the operating temperatures of high temperature-SOFC (1000–1400 K). Under cell operating conditions the hydrogen should be removed in the power production step (reaction 3) and water produced. This will unbalance reaction 7 such that, by LeChatelier's principle, the reaction will be driven to the right producing more hydrogen and carbon dioxide.

2.2. Catalysts

The catalytic activity of the anode material used can influence the type of fuels that can be processed by the cell, the temperature at which the cell is operated, and the active lifetime of the cell. One of the major concerns with the long-term operation of SOFCs is the deactivation of the nickel anode either by sintering, poisoning by sulphur (when running on natural gas) and the formation of carbonaceous deposits (when using hydrocarbon fuels) [25,26]. In recent years supported nickel catalysts have been commonly used in industrial steam reforming. Other metals have shown comparable and even high activity for steam reforming, these include Co, Pt, Pd, Ru and Rh. Some of the precious metals mentioned show much higher activity per unit weight than Ni, but Ni is much cheaper and has sufficient activity to provide a more economic option [27]. Unfortunately the reforming of hydrocarbons over nickel catalysts leads to carbon deposition [28–30], which in time deactivates the catalyst and renders it inactive. Sintering of the catalyst and metal-support interactions can also cause deactivation. It is also well known that carbon deposition can be mitigated using high steam to carbon ratio (SC).

One of the attractive features of SOFCs is their ability to oxidize methane efficiently without the need for an external reformer, but the problem of carbon deposition must be fully overcome for this to be economically viable. As mentioned above, the nickel surface in Ni/YSZ anode can catalyze the steam reforming reaction in a similar way to the previously mentioned industrial catalyst. In fact, several theoretical and experimental studies proved the feasibility of SOFC direct internal reforming. Aropornwichanop et al. [6] developed a theoretical study, investigating an anode supported fuel cell with direct internal reforming of ethanol, achieving a power density of 0.51 W cm^{-2}. A similar numerical study was performed by Janardhanan and Deutschmann [5], investigating the performance of a planar SOFC under direct internal reforming conditions. Authors of this study concluded that direct internal reforming may lead to cost reduction and increased efficiency by effective utilization of waste heat. Regarding the experimental activities on direct internal reforming SOFC, two interesting studies can be cited. The former [8] investigates a LSM/YSZ/Ni-YSZ SOFC, equipped with a Ir-CeO_2 layer, fed by methane. The cell was first successfully operated by humidified methane. Then, it was fed by dry methane at 900 °C and 0.60 V, showing a deterioration of performance, not due to carbon deposition. The latter study [7] presented an experimental analysis of a planar doped-ceria Ni-YSZ/3YSZ/Ni-GDC SOFC fed by simulated bio-methane and bio-hydrogen. The authors of this study concluded that, in case of bio-methane, carbon deposition could be avoided adding oxidant to the fuel stream in order to promote conversion into hydrogen. In case of bio-hydrogen the additional oxidant was not required.

Under the operating conditions, industrial steam reforming catalysts and SOFCs carbon deposition is thermodynamically favorable [31]. Carbon deposition on the anode is thought to occur via a variety of mechanisms which will be discussed in more detail in the next section [32,33]. The principal routes to carbon deposition are the Boudouard reaction (reaction 10), the catalytic methane decomposition (reaction 8) and the direct reduction of CO species at the nickel surface (reaction 9). Carbon deposition can be limited, by adjusting the fuel mixture supplied to the reforming catalyst or SOFC anode. For maximum cell performance and minimum cost, H_2O partial pressures (p_{H_2O}) must be kept low. However, unfortunately these conditions promote carbon deposition causing degradation of the industrial catalyst and destroying the anode in SOFCs. High p_{H_2O} give little or no carbon deposition, but due to the high p_{H_2O} in the fuel, the cell performance is inhibited and the extra cost of producing water vapor makes this industrially unfavorable [34].

Little is known about the kinetics of steam reforming on Ni/YSZ cermets but it is hoped that knowledge of the kinetics may help optimization of anode design in the future. Another problem that can arise with direct internal reforming is large temperature gradients along the anode. As noted above the steam reforming reaction is endothermic. This can cause the anode at the fuel inlet to cool, severely inhibiting electrochemical performance, and setting up potential differences across the anode itself, as the conductivity of the anode is dependent on temperature [34].

2.3. Carbon formation and deposition

One of the major problems associated with the steam reforming of hydrocarbons over nickel based catalysts is that of carbon deposition. Hydrocarbons that are introduced to the catalyst at the operating temperatures involved, will spontaneously decompose to form surface adsorbed carbon and gaseous hydrogen, via reaction 8, in the case of methane. This reaction is referred to as thermal cracking or methane decomposition [35]. The introduction of steam into the reactant stream inhibits this reaction, reducing carbon deposition and promoting the methane steam reforming process. The steam reforming process does however have associated side reactions, especially when the steam to fuel ratio is less than stoichiometric [35]. The Boudouard reaction 10 is a disproportionantion of CO. This reaction is also catalyzed by nickel at high temperatures and can be controlled by manipulation of feed gases. As water content is increased, the WGS reaction favors the production of CO_2, thus inhibiting the Boudouard process as stated earlier. The other possible route for the formation of surface carbon is the direct reduction of CO species at the nickel surface (reaction 9). This reaction is also inhibited by the addition of steam [35]. The carbon deposited during these reactions can, over time, deactivate the catalyst and render it useless for its intended purpose. This observed deactivation can be caused by:

- Fouling of the metal surface;
- Blocking of active catalytic sites;
- Destruction of the catalyst support.

Table 2
Electrical conductivity data for CeO_2–Ln_2O_3.

	Mol%	Conductivity (S cm^{-1})		Activation energy (kJ mol^{-1})	
		700 °C	500 °C		
Sm_2O_3	1010	3.5×10^{-2}4.0 $\times 10^{-2}$	2.9×10^{-3}5.0 $\times 10^{-3}$	68	75
Gd_2O_3	10	3.6×10^{-2}	3.8×10^{-3}	70	
Y_2O_3	10	1.0×10^{-2}	0.21×10^{-3}	95	
CaO	5	2.0×10^{-2}	1.5×10^{-3}	80	

The deactivation of the catalyst by any one of these mechanisms can occur rapidly in unfavorable conditions. Thus the need for understanding of these processes is of major importance [36]. Surface carbon and coke are defined conventionally by the origin of the carbon deposit. The decomposition of hydrocarbons such as methane (reaction 8) leads to the formation of cokes, whereas, the disproportionation of CO (reaction 10) gives carbon [36]. The nature of coke deposits on a catalyst can vary from graphite species to high molecular weight hydrocarbons, according to the reactions conditions the coke was deposited under [37,38].

The high temperatures involved in steam reforming could potentially lead to gas phase reactions producing carbonaceous intermediates, which then condense onto the catalyst surface to form coke. These reactions rely on free radical polymerizations to occur in the gas phase, which can easily be controlled by the addition of water to the gas phase [37].

The vast majority of coke formation occurs at the catalyst surface. Carbonaceous deposits can be divided into three main types: amorphous, filamentous and encapsulating graphitic structures [38,39]. Amorphous carbon is thought to be formed via condensation and polymerization reactions, and is the product of thermal processes during steam reforming. There is a possibility that this deposit has significant hydrogen content, however, as the reaction temperature is increased the associated hydrogen content will decrease as dehydrogenation reactions become more thermodynamically favorable [38]. The formation of filamentous and graphitic carbon forms has been the subject of much discussion and is now thought to proceed only in the presence of a catalyst.

Early studies by Rostrup–Nielson concluded that during steam reforming, three different carbon species were formed: the aforementioned filamentous carbon was formed above 723 K, encapsulating hydrocarbon films formed below 773 K which dehydrogenate at higher temperatures and pyrolytic carbon above 873 K [39]. However, one of the main products of steam reforming is CO which will interact with the nickel surface to produce further carbon [40].

Carbon deposits from both the steam reforming reaction and the decomposition of CO and other carbon containing species may involve the generation and transformation and ageing of several different carbon species. There are several carbon species that must be considered within the system. Low density filamentous carbon and graphitic species have both been observed at elevated reaction temperatures. However it must be noted that prolonged exposure to higher temperatures can make the filaments and amorphous film species become more graphitic [36].

3. Doped ceria SOFC

The properties of a catalyst can be enhanced by careful preparation and changing the reaction environment, but the simplest way to enhance a catalyst is the introduction of additives or promoters [41]. Industry has utilized considerable resources in developing steam reforming catalysts which are resistant to coke formation at or near stoichiometric reaction ratios. Sulphur passivated, potassium doped and noble metal catalysts have all shown kinetic resistance to coke formation. However, high cost of materials has limited the widespread application of noble metal catalyst [42], but despite lower activities potassium doped catalyst are commonly used. Similarly a major obstacle to the long-term feasibility of solid oxide fuel cells as a viable energy source is that of carbon deposition or coking during high temperature reforming of hydrocarbon fuels.

Increases in resistance to coking have been observed after the addition of 3–15 wt% of the oxides of certain metals [41]. These metal oxides include those of uranium, lanthanum and cerium. The introduction of additives can affect both the overall activity of the catalyst and its active surface area [41].

As known, the life expectancy of a fuel cell powered by direct internal methane reforming gas is limited to few hours before carbon deposition blocks the cell and causes it to fail. For commercial purposes this situation needs to be dramatically improved.

It is possible to improve the situation by changing the flow rates and running temperature of the fuel cell system but a more perfect solution is to alter the chemistry within the fuel cell by the use of an appropriate catalyst.

The chemistry within a methane reforming fuel cell is complex with 10 major reactions taking place. This chemistry needs to be fine tuned to the fuel cells advantage. This can be achieved by one of 2 major ways:

a. Improve the rate of the reforming reactions, leaving less methane available for pyrolysis or other carbon forming reactions.
b. Lower the rate of the carbon forming reactions.

The main drawback with the use of nickel as a reforming catalyst is that it also promotes the formation of carbon. This leads to attempts to modify the nickel with various dopants to either increase the reforming reactions or decrease the carbon forming reactions. The attempts to decrease the carbon forming reactions usually revolve around lowering the activity of the nickel, which affects the carbon forming reaction more than the reforming reactions [43,44].

Many different metal and metal oxide dopants have been employed to improve the reforming reactions catalytically and limit carbon deposition during methane reforming [45,46]. One of the more commonly used additive to nickel is cerium oxide (ceria) [47,48]. Cerium oxide (ceria) is an excellent catalyst for oxidation reactions both through its ability to exist in two reasonably stable electronic configurations, and also by its ability to donate and accept oxygen. Therefore, this material was employed for the construction of the micro-tubular SOFC prototype under test, as explained in detail in the next section.

Ceria-based electrolyte seem to have higher electrolyte conductivity and moreover, when ceria is used as anode dopant, show higher resistance at the carbon deposition phenomena. Furthermore this fuel cell operating at intermediate temperature show lower start up time, extending the lifetime of the SOFC stack, reducing cost by allowing the use of metal materials, and decreasing the degradation of SOFC and stack materials [4].

Reviews on the electrical conductivity and conduction mechanism in ceria-based electrolytes have been presented by Mogensen et al. [4] and Steele [4]: CeO_2–Gd_2O_3 and CeO_2–Sm_2O_3 show an

ionic conductivity as high as 5×10^{-3} S cm^{-1} at 500 °C, corresponding to 0.2 Ω cm^2 ohmic loss for an electrolyte of 10 μm thickness (Table 2). These compositions are attractive for low temperature SOFCs.

Ceria-based oxide ion conductors are reported to have purely ionic conductivity at high oxygen partial pressures. At lower oxygen partial pressures, as prevalent on the anode side of an SOFC, these materials become partially reduced. This leads to electronic conductivity in a large volume fraction of the electrolyte extending from the anode side. When a cell is constructed with such an electrolyte with electronic conduction, electronic current flows through the electrolyte even at open circuit, and the terminal voltage is somewhat lower than the theoretical value.

A SOFC with ceria-based electrolyte should be operated at temperatures below about 600 °C to avoid efficiency loss due to electronic leakage. Successfully ceria-based electrolytes have been used in SOFCs operating at 550 °C and lower.

4. Experimental

4.1. Solid oxide fuel cells test stand

The performance of the fuel cells was analyzed using an in-house SOFC test stand. This experimental setup was extensively presented in [23]. Therefore, in this section only a brief description of this equipments is included.

The stand is based on a *Carbolite vertical tubular Furnace* which is equipped with an advanced set-point programming temperature controller, used to stabilize the output power and temperature, and ramp rate temperature control (a ramp rate of 1.5–2.0 °C min^{-1} was used both for heat-up and cool down).

The stand is also equipped with a *Chroma 6310 series Electrical Load*. This system is capable of drawing a fixed amount of current from the fuel cell and thus measuring the corresponding output voltage, both under static and dynamic condition. In addition, a *Gamry 600 Potentiostat/Galvanostat* was employed in order to evaluate the determine the typical EIS (electrochemical impedance spectroscopy) shape.

The test stand also includes hydrogen, carbon monoxide, carbon dioxide, methane and nitrogen pipe lines. All the pipe lines are equipped with a "bubbler system" capable to introduce different quantities of steam inside the gas mixture entering the cell. This system is used during the fuel cell polarization curve measurement to introduce a small amount (2–3% of total mass flow) of steam in the hydrogen stream in order to reach a more stable trend of the voltage during the current drawing. In addition, during the tests with CH_4 and CO, the steam flow is regulated in order to achieve the desired steam to carbon ratio. The operating principle of this device is simple: the gas flow, coming from the gas flow meter, is bubbled inside the steel tank (filled with water), and subsequently a small amount of water evaporates, depending on the water saturation pressure, for a given water temperature. The water tank is surrounded by a heating type with adjustable thermostat, capable to control the water temperature, that allows to fix properly the amount of required steam in the gas stream. The relationship between the water saturation pressure and the temperature is represented by the Clausius-Clapeyron relation that could be approximate by the Magnus formula.

Each gas pipeline is also equipped with a MKS Thermal Mass Flow Meters (type 179) linked to a MKS mass flow controller (MFC) capable of setting the expected volume flow. Each pipeline is linked to a single cylinder containing a different gas. On the top of each cylinder a pressure reducer (regulator) was installed in order to achieve values of pressure inside the pipes higher than the environmental one (20 psi—138 kPa).

Finally, a PC data acquisition system was used in order to control the instrument and save the data produced during the experiments.

4.2. Fabrication process

Micro-tubular SOFCs were developed with diameters in the millimeter and sub-millimeter ranges for intermediate temperatures operation between 450 and 550 °C [23]. In this study, micro-tubular SOFCs measuring 1.8 mm in diameter and 3.0 cm in length (with active cathode length of 9 mm, whose active cell area is estimated to be 0.50 cm^2) were fabricated. The micro-tubular SOFC used is anode supported, consisting of a NiO and $Gd_{0.2}Ce_{0.8}O_{2-x}$ (GDC) cermet anode, thin GDC electrolyte, and a $La_{0.6}Sr_{0.4}Co^{0.2}Fe_{0.8}O_{3-y}$ (LSCF) and GDC cermet cathode.

Micro-tubular SOFCs were fabricated using traditional extrusion and coating techniques in a process similar to that described by Suzuki et al. [18], with changes to fabrication processes noted in [23]. Anode slurry was prepared and consisted of NiO powder, GDC powder, and cellulose as the binder. The GDC electrolyte slurry is composed of the same GDC powder described above, and organic ingredients such as binder (poly vinyl butyral), dispersant (fish oil) and solvents (toluene and ethanol). The desired electrolyte thickness was achieved through multiple electrolyte coatings and subsequent sintering at 1450 °C. Next, the electrolyte coated anode tubes were dip-coated in cathode slurry consisting of $La_{0.6}Sr_{0.4}Co_{0.2}Fe_{0.8}O_{3-y}$ (LSCF) and GDC powder, and organic ingredients similar with those of the electrolyte slurry. The cathode dip-coated tubes were dried in air and sintered, to complete the fuel cell fabrication.

The single cell is also equipped with a specific support, which is capable of: (i) sustaining the fuel cell when it is mounted in the furnace; (ii) allowing the gas distribution on the anode and cathode sides; (iii) assuring the electrical connection with the electrical load and potentiostat.

Each tube was equipped with four 0.5 mm silver sensor wires attached for collecting current for the anode and cathode sides. The anode electrical connection was realized using two long silver wires fixed using nickel paste. A silver wire was wrapped around the tubular fuel cell (on the cathode), as a reel, and fixed with silver paste for the cathode electrical connection. The silver paste and nickel paste were brush painted on the cathode and anode surfaces respectively to reduce the contact resistance between the silver sensor wires and the electrode surfaces.

The four current collecting wires from the cell were connected to the impedance analyzer (Gamry 600) and the electrical load (Chroma 6310 series) at operating temperature ranges between 450 and 550 °C. Individual cells were run using different fuels:

- humidified hydrogen gases (2–3% of H_2O)
- H_2–CO–H_2O mixtures (S/C = 2–3)
- H_2–CH_4–H_2O mixtures (S/C = 2–3)

The cathode side (outside surface of tube) was exposed to atmospheric conditions. The type of air pump normally used for small aquariums was used to facilitate new air into the bottom of the micro-tube furnace to assist convective flow of air through the furnace. The overall system is shown in Fig. 1. Details regarding system arrangement are diffusely given in Ref. [23].

5. Results of the tests

The main aim of this study was the analysis of the micro-tubular SOFC electrochemical performance degradation when fed by carbonaceous fuels. In particular, the goal of the study is the evaluation of the GDC components of inhibiting the carbon deposition phe-

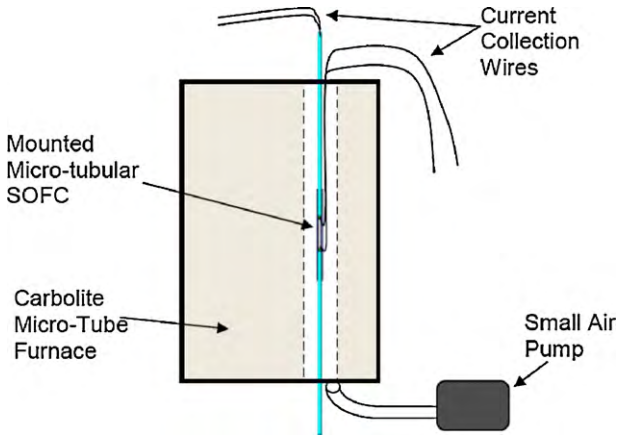

Fig. 1. Setup of micro-tubular SOFC inside of a vertical micro-tube furnace [23].

nomena and the resistance of the cell to the thermal, mechanical and chemical stresses in different load cycles. To this scope, four different experimental tests were performed: (i) load cycles using H_2–CH_4 mixtures gradually increasing in CH_4 content (S/C = 2–3); (ii) load cycles H_2–CO mixtures gradually increasing in CO content (S/C = 2–3); (iii) long-term test fed by humidified H_2; (iv) long-term test fed by H_2–CO mixtures (S/C = 2–3). Load cycles were performed scanning the polarization curve starting from the OCV down to the limiting current density, according to the procedure described in detail in Ref. [23]. Note that, for each of the four above cited experimental tests, a new blank cell was employed.

Long-term experiments, showing cell performance degradation in case of humidified CH_4 fuel mixtures, were not shown, since the cells failed after few hours of operation, as a consequence of the carbon deposition phenomenon.

The cells used were 3 cm long (0.9 cm of reactive area length) with a 1.8 mm diameter for an active cell area of 0.5 cm^2. The experiments were performed on the basis of the results achieved in previous studies regarding the same type of cell, fed by hydrogen [23]. Here, the authors concluded that the maximum power density (which must be maximized, according to the goal of the study) is achieved at 550 °C and 25 S cm^3 h^{-1} H_2 flow rate. Higher operating temperatures could not be acceptable for the material constraints of the cell under investigation, as discussed in the previous section. In addition, higher temperatures would determine longer start up and shut down periods and also higher thermal stresses, which should be both limited, as mentioned in the introduction. Furthermore, high volume flows would determine dramatically low fuel utilization factors [23]. Therefore, the operating temperature was set at 550 °C, whereas the nominal H_2 flow rate was 25 S cm^3 h^{-1}. S/C was always kept higher than 2. In fact, in a theoretical complete steam methane reforming process, 2 moles of steam are required for each mole of CH_4 reacting. However, the real amount of steam required to support the reforming reaction is significantly lower, due to the kinetics of reforming process [4]. Thus S/C = 2 is higher than the corresponding stoichiometric value. In addition, this limit is commonly considered as the minimum value required in order avoid carbon deposition [4]. As regards the other boundary experimental conditions, further details can be found in Ref. [23].

5.1. CH_4–H_2–H_2O mixtures

This test was performed using different mixtures of methane, hydrogen and water as fuel. The test was started using a stream of 25 S cm^3 h^{-1} of hydrogen as fuel for 5 load cycles in which the polarization curves were plotted scanning cell potential from OCV to the lowest value of cell voltage. The results of these tests are shown in Fig. 2, where both voltage and power density (p) versus current density (i) are plotted. This graph shows results compliant with those ones reported in a recent study published by the authors [23], since the cell under test was capable to achieve an OCV approximately of 0.84 V, whereas the power density, at 2.0 A cm^{-2}, was approximately 0.72 W cm^{-2}. In addition, the same figure also clearly shows a slightly perceptible deviation of the electrochemical performance of the cell, with respect to the first load cycle. This deviation is very scarce at low current density (<1%) whereas it may increase significantly increase at higher current densities, where the operating voltage may be 5% lower than the original value. This result suggests that – using only hydrogen as fuel – the cell performance is quite stable if the cell operates at current density lower than 0.40 A cm^{-2}, whereas a faster electrochemical reaction may lead to a not negligible increase of electrochemical losses. The trend shown in Fig. 2 should not be surprising. In fact, a number of phenomena, others than carbon deposition, may contribute to the performance degradation of this kind of fuel cell. In particular, authors postulate that the main source of this degradation should be identified in some electrical problems due to the fact that, after some load cycles, the electrical wires may lose the intimate contact with the

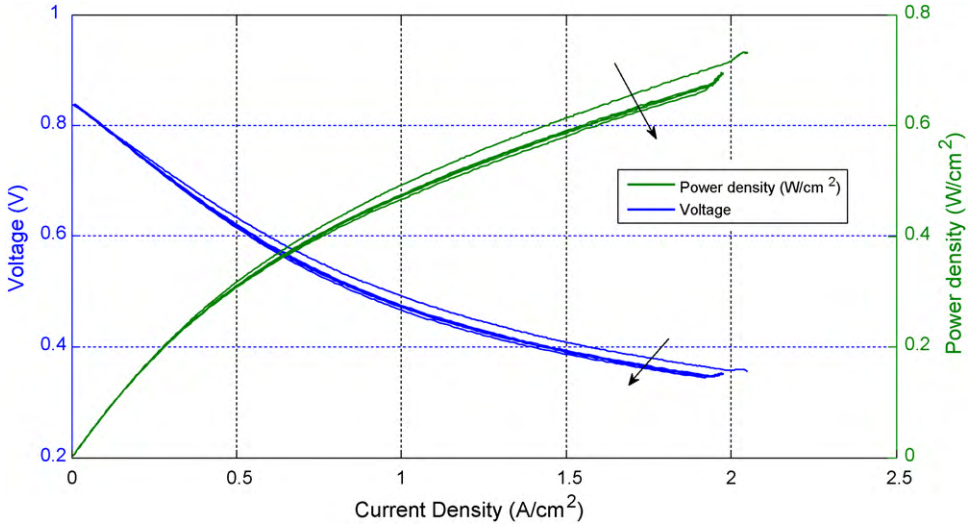

Fig. 2. V–i and p–i curves, 5 load cycles, 25 S cm^3 h^{-1} H_2.

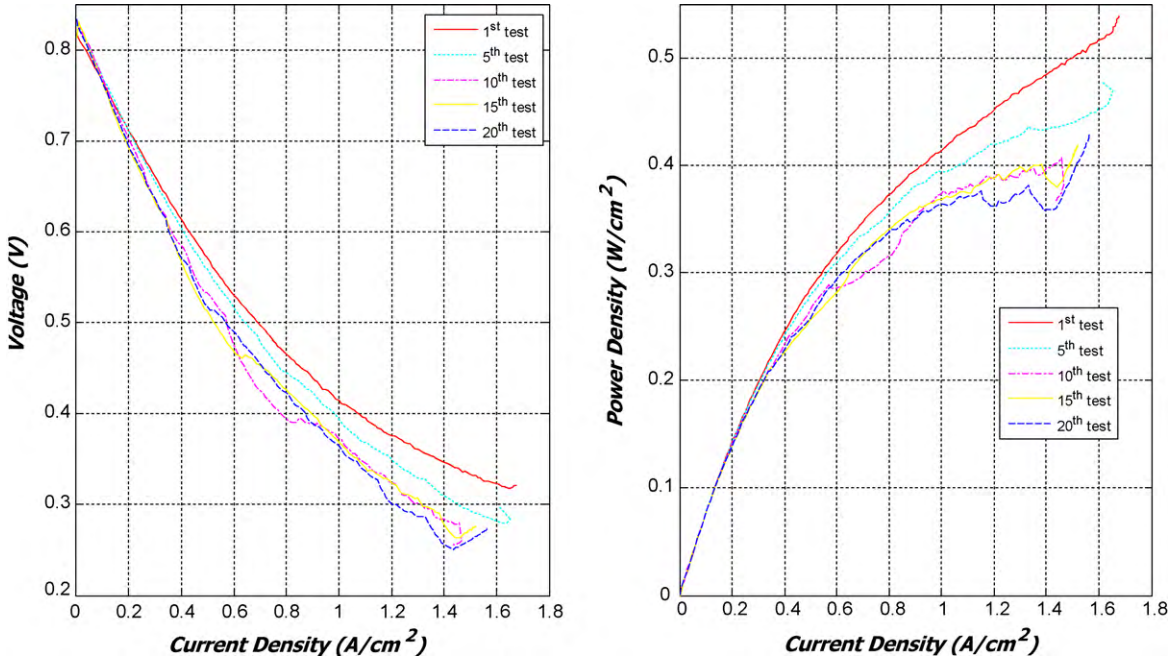

Fig. 3. *V–i* and *p–i* curves, 20 load cycles, 20 S cm^3 h^{-1} H_2 + 1.25 S cm^3 h^{-1} CH_4.

external surface of the micro-tubular SOFC, increasing the ohmic losses. In addition, micro-tubular SOFC under investigation are still excessively subject to thermal, mechanical and electrochemical stresses, showing a significant fragility. Such phenomena may promote cracks and micro-cracks in the SOFC structure, leading to fuel cross over and consequently to a loss in cell gross electrical power production. Finally, a variation in material microstructure may also occur, determining a deviation from the original electrochemical performance. These assumptions, postulated by the authors on the basis of empirical investigations, will be subsequently validated in future studies using more accurate techniques (SEM, dilatometry, etc).

After these first 5 load cycles fed by humidified hydrogen, the cell under investigation was fed by a gas mixture of methane and hydrogen with methane content growing proportionally with the reduction of hydrogen. Thus, the cell was tested with a mixture of 20 S cm^3 h^{-1} of H_2 and 1.25 S cm^3 h^{-1} of CH_4. The selection of such flow rates comes from the consideration that a stoichiometric steam reforming of 1 S cm^3 h^{-1} of methane produces 4 S cm^3 h^{-1} of H_2. Hence, the selected flow rates are "equivalent" to the value

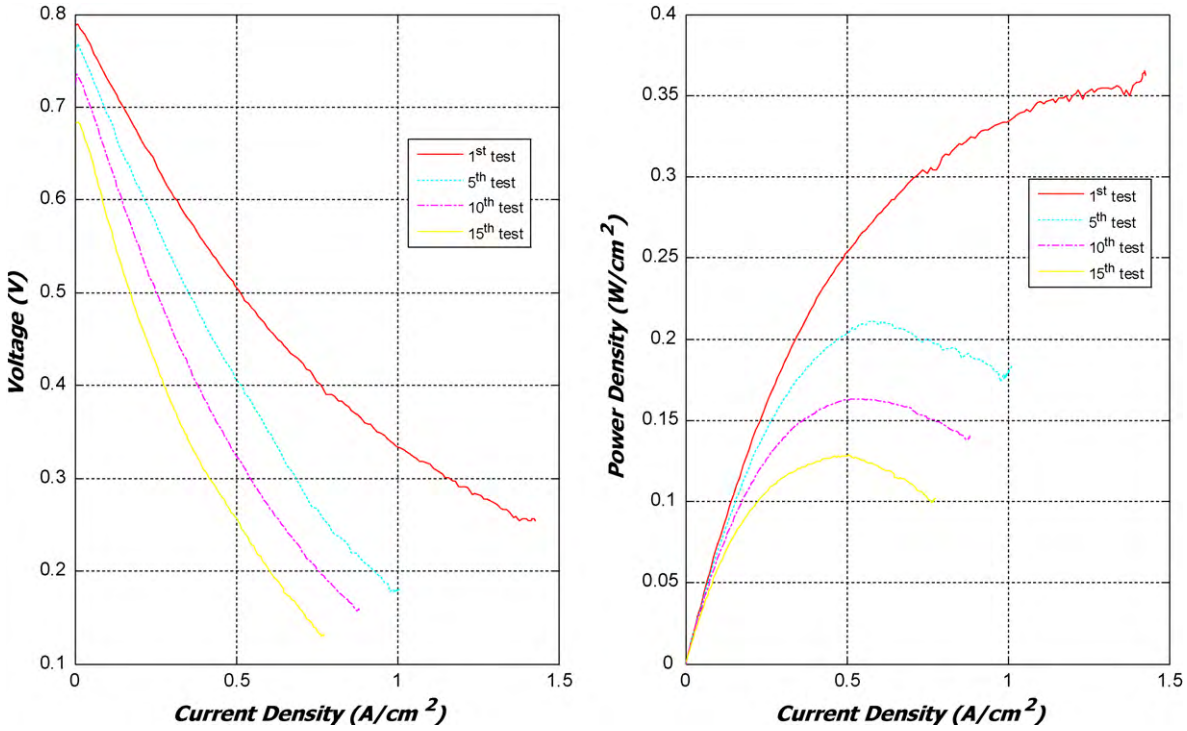

Fig. 4. *V–i* and *p–i* curves, 15 load cycles, 15 S cm^3 h^{-1} H_2 + 2.5 S cm^3 h^{-1} CH_4.

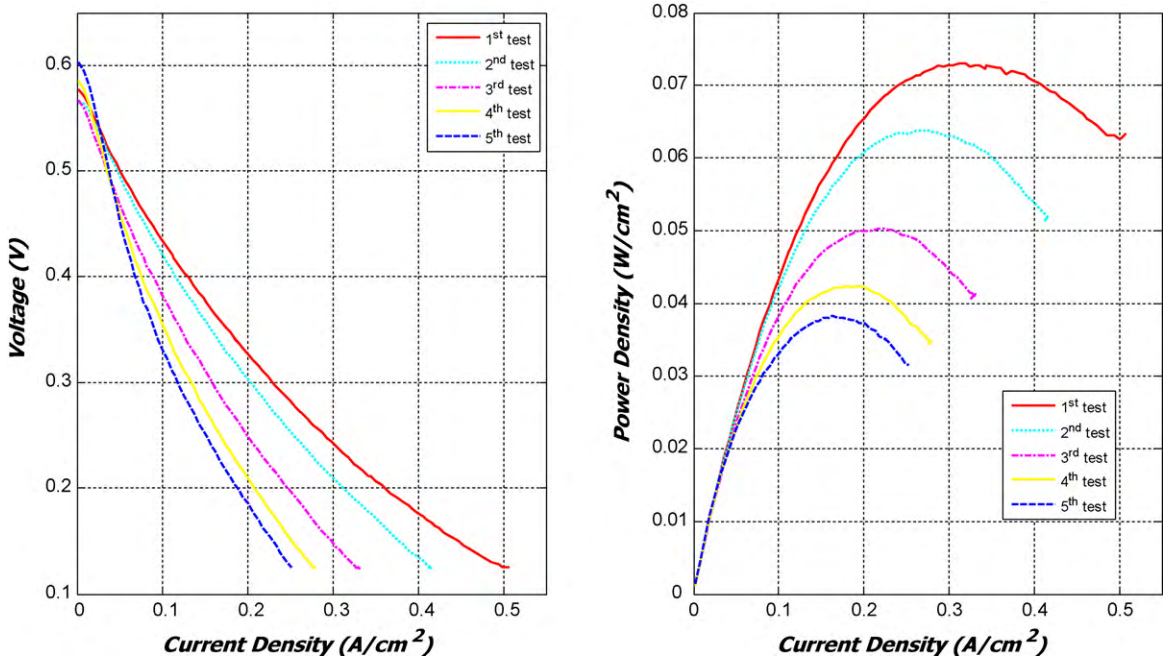

Fig. 5. *V–i* and *p–i* curves, 5 load cycles, 5 S cm^3 h^{-1} H_2 + 5 S cm^3 h^{-1} CH_4.

of 25 S cm^3 h^{-1} of H_2 used in the first 5 tests. In addition, an adequate flow of steam was also added in the mixture in order to achieve a steam to carbon ratio (S/C) higher than 2.0. This value can be achieved simply by regulating properly the bubbler temperature. Using the above mentioned CH_4, H_2 and H_2O flow rates, 20 load cycles were performed. The results of this test are shown in Fig. 3. This graph displays that the performance degradation is in the same order of magnitude with respect to the case of pure hydrogen as fuel. However, some additional conclusions can be drawn. At 1.0 A cm^{-2}, the power density achieved during the first test by pure hydrogen was approximately 0.49 W cm^{-2}. During the 1st and the 20th tests, by the considered H_2–CH_4 mixture, the values of power densities – at 1.0 A cm^{-2} – are respectively 0.41 and 0.36 W cm^{-2}, showing a significant decrease. In addition, a slight reduction of the OCV can also be observed. In this case, the reduction of voltage and OCV may be mainly ascribed to the diluted fuel feeding the cell. In addition, the above mentioned degradation phenomena also contribute to voltage and power density decrease. Furthermore, in this case there is no experimental evidence that this degradation is due to carbon deposition. Thus, it may be concluded that, using this combination of CH_4 and H_2 flow rates, the carbon deposition phenomena may be a possible additional source of degradation, although its magnitude may be considered still marginal.

The subsequent experiment was performed using a mixture of 15 S cm^3 h^{-1} of H_2 and 2.5 S cm^3 h^{-1} of CH_4 ("equivalent" to 25 S cm^3 h^{-1} of H_2), and S/C2–3, for 15 load cycles. The results of these experiments are shown in Fig. 4. Here, it can be clearly seen that the degradation is much more pronounced with respect to the previous gas mixture. The OCV significantly decreases and the maximum power density (15th load cycle) is approximately

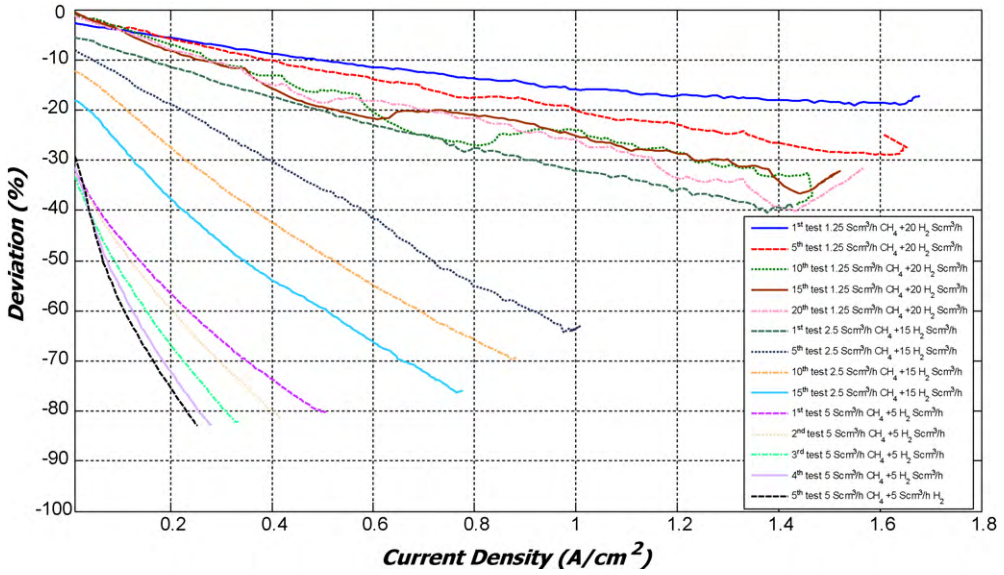

Fig. 6. Comparison between the different load cycles by CH_4–H_2 mixtures.

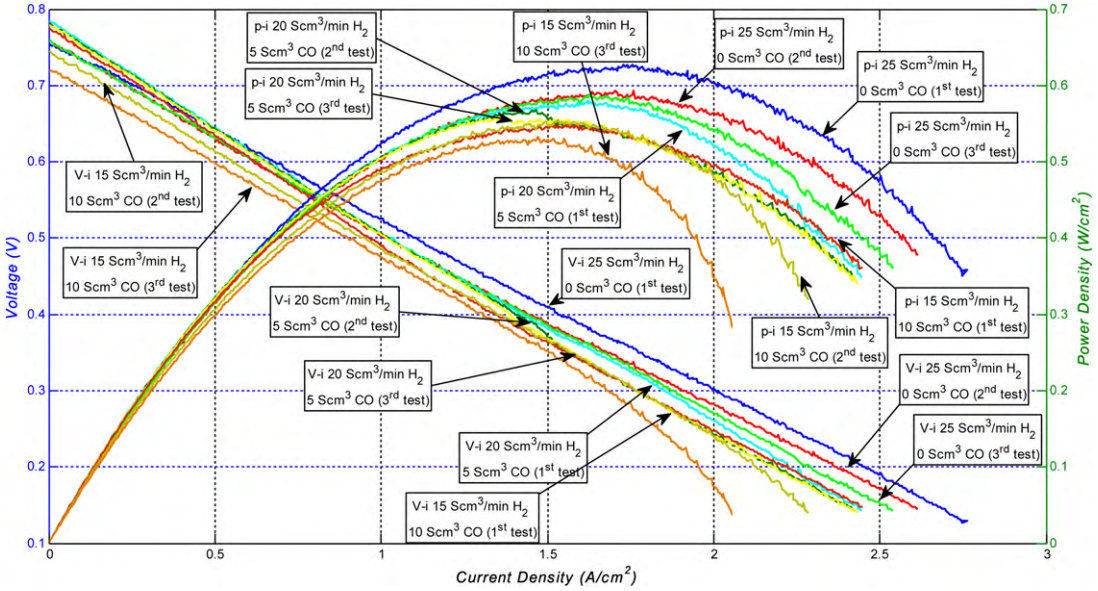

Fig. 7. *V–i* and *p–i* curves, 9 load cycles, 15–25 S cm^3 h^{-1} H_2 + 0–10 S cm^3 h^{-1} CO.

0.12 W cm^{-2}. In this case, the magnitude of the degradation is dramatically significant. In addition the rate of the increase of performance degradation is dramatically higher than the one reported using H_2 as fuel [23,49]. Therefore, the voltage and OCV reduction cannot be considered only as a simple consequence of fuel dilution and of the above mentioned degradation phenomena. Thus, authors postulated that in this experiment carbon deposition was occurring. This assumption, was next validated by the subsequent long-term experiments (Section 5.3) showing that cells, fed by CH_4 mixtures, completely failed after few hours of operation although the same cell, fed by humidified hydrogen, showed a good performance stability.

This is also confirmed by the last test (Fig. 5), which was performed using a mixture of 5 S cm^3 h^{-1} of H_2 and 5 S cm^3 h^{-1} of CH_4 ("equivalent" to 25 S cm^3 h^{-1} of H_2), and S/C = 2–3, for 5 load cycles. In this case, the carbon deposition has almost inhibited the electrochemical reactions. In fact, OCV is lower than 0.60 V, the maximum current density (5th load cycle) is approximately 0.25 A cm^{-2} and the maximum power density is lower than 0.040 W cm^{-2}.

For a better comparison, the deviations of the considered 40 tests by the CH_4-H_2 mixtures, with respect to the first test by H_2, are shown in Fig. 6. Here, the effect of the carbon deposition is dramatically clear, showing a dramatic increase of the rate of performance degradation. Additionally, it can be also observed that the first gas mixture does not significantly affect the OCV, whereas the OCV significantly decreases with second (approximately 20%) and third gas mixture (approximately 35%), showing the dramatic effects of the carbon deposition.

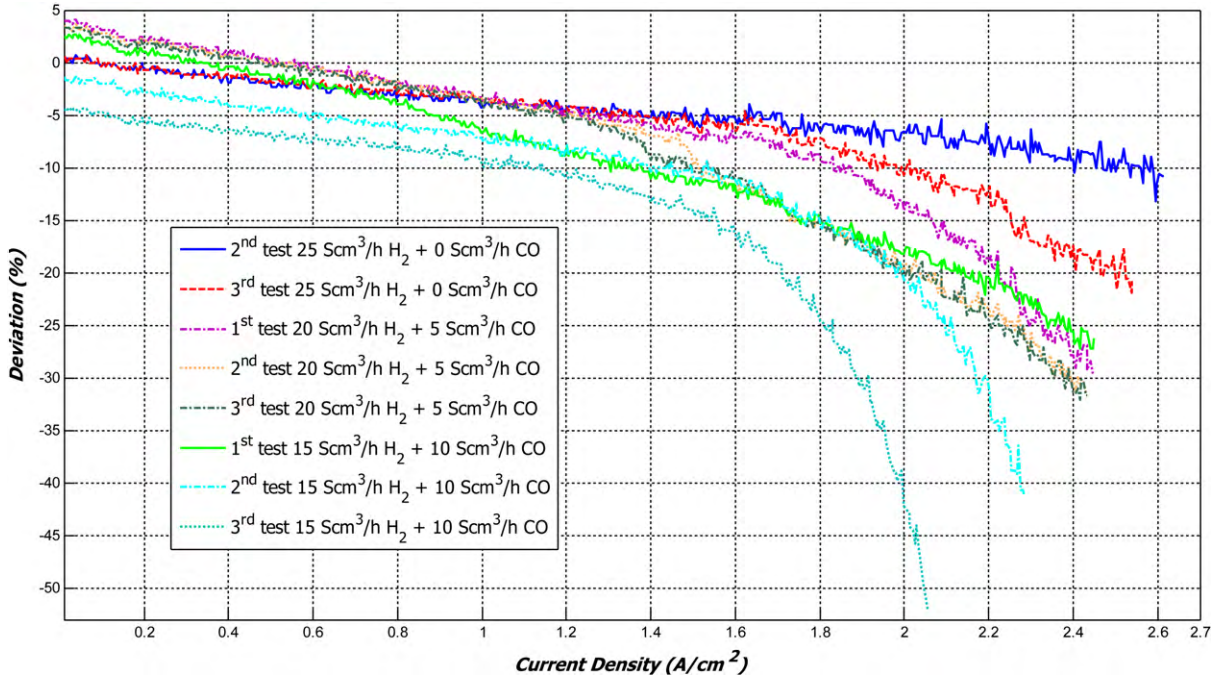

Fig. 8. Comparison between the different load cycles by CO–H_2 mixtures.

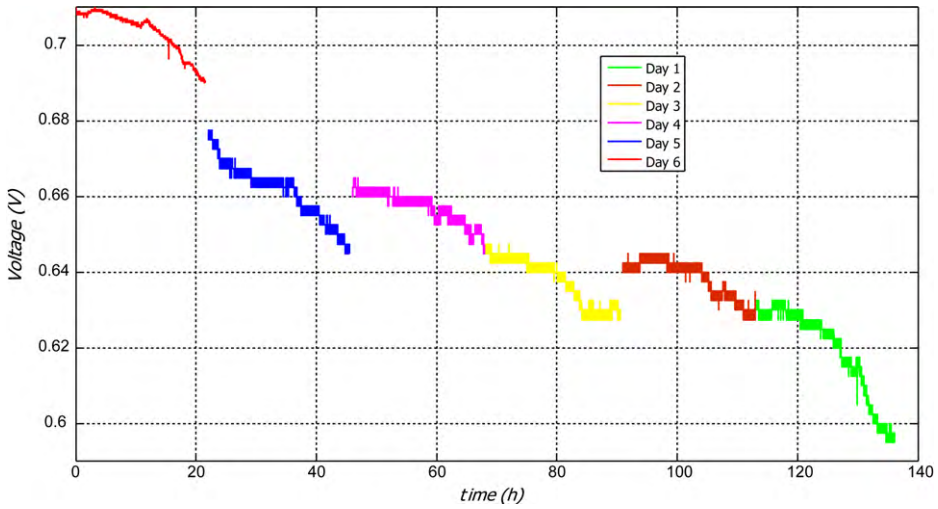

Fig. 9. Long-term experiment, 25 S cm^3 h^{-1} H_2, i = 0.40 A cm^{-2}.

Results of this first experiment are not encouraging since it can be deduced that ceria does not inhibit, as expected, carbon deposition phenomena, since it only contributes to delay the phenomena. In fact, authors postulated that the action of nickel included in SOFC materials catalyzes carbon deposition more rapidly than ceria inhibition. This circumstance is validated by several previous studies [4] investigating carbon deposition on SOFC materials. In addition, the carbon deposition reactions are also "catalyzed" by the slowness of the reforming reactions. In fact, at 550 °C the reforming reaction are far from the equilibrium, so that a lot of CH_4 and CO are available for reactions 8, 9 and 10, determining carbon deposition. Recent studies showed that carbon deposition may be mitigated using cooper-based anodes. In fact, in catalytic technology the advantages of copper composites with ceria are recognized [4]. Partial reduction of copper oxide when exposed to fuel at elevated temperature, and the resulting redox properties, permit exchange of oxygen between the lattice and the gas phase, with availability for surface reactions. A copper–ceria composite anode [4] is a recent promising initiative. The difficulty of sintering a copper composite was avoided by forming a porous zirconia skeleton on a dense electrolyte substrate of the same material, then introduction of copper and cerium as their nitrate salts in solution, followed by drying and pyrolysis, similar to a procedure already demonstrated for anode and cathode catalysts [4]. Co-insertion of the two cations is possible since copper does not form a solid solution in ceria so the two phases remain separate as required for functionality of the electrode. The performance of cells using this zirconia-supported copper–ceria composite, show that the power density with methane fuel is significantly lower than that with hydrogen. There are also evidences of the stability of the composite anode, in contrast to a nickel cermet where the fuel cell operation is suppressed irreversibly within 30 min by the carbon accumulation. The ceria–copper system is now being further investigated for the direct oxidation of higher hydrocarbons [4].

5.2. CO–H_2–H_2O mixtures

This test was performed using different mixtures of carbon monoxide, hydrogen and water as fuel. The test was started using a stream of 25 S cm^3 h^{-1} of hydrogen as fuel for 3 load cycles, using an adequate steam flow in order to achieve S/C = 2–3. Then, hydrogen was gradually replaced by CO. Assuming that, for a stoichiometric water gas shift reaction, 1 S cm^3 h^{-1} of CO is converted in 1 S cm^3 h^{-1} of H_2, in the subsequent mixtures the sum of hydrogen and carbon monoxide flow rates are always "equivalent" to the original 25 S cm^3 h^{-1} of H_2. In fact, after the first 3 load cycles by humidified hydrogen, mixtures of 20 S m^3 h^{-1} of H_2 and 5 S cm^3 h^{-1} of CO were employed for 3 load cycles. Finally, the test was concluded by 3 load cycles, consisting of 15 S cm^3 h^{-1} of H_2 and 10 S cm^3 h^{-1} of CO. The results of these tests are shown in Fig. 7. Here, it is clearly shown that the performance of the fuel cell is much more stable with respect to the corresponding test by methane. In fact, in this case performance degradation is less significant. The graph shows that at 1.0 A cm^{-2}, during the first load cycle by hydrogen, the power density was approximately 0.52 W cm^{-2}, whereas the same parameter is 0.50 W cm^{-2}, both during the 3rd load cycle by H_2 the during the 3rd load cycle by the second gas mixture. Finally, during the 3rd load cycle of the last mixture, the power density was 0.47 W cm^{-2}. Therefore it may concluded that, at reasonably low values of cell current density, cell electrochemical degradation is marginal. These results are more clearly displayed in Fig. 8, where the deviation of the experiments with respect to the 1st load cycle by H_2 are reported. Here, it is clearly shown that, for current densities lower than 1.0 A cm^{-2}, the degradation is lower than 10%, even when the cell is fed by 15 S cm^3 h^{-1} of H_2 and 10 S cm^3 h^{-1} of CO, at the 3rd load cycle. Conversely, at high current densities, the deviation of the cell electrochemical performance, may also exceed 40%. The results can be interpreted postulating that, at the operating conditions, the ceria-based SOFC materials are capable to inhibit reactions 9 and 10 much more efficiently than reaction 8.

5.3. Long-term tests

Finally, long-term tests of the selected micro-tubular cell, fed by H_2 and H_2–CO–H_2O mixtures were performed, in order to evaluate the electrochemical degradation of the ceramic materials and to establish the capability of this cell to resist to carbon deposition, on longer time basis. As above mentioned, results of long-term tests of the cell fed by CH_4 mixtures are not reported, since the cells completely failed after few hours of operation.

On the basis of the experiments described in the previous sections, a first test was performed using only hydrogen as fuel, in order to evaluate the stability of the materials employed for the fabrication of the fuel cell. In other words, this test aimed at evaluating the degradation shown in Fig. 2, on a longer operating period. Moreover, a current density of 0.4 A cm^{-2} was set, which is a typical operating value of micro-tubular SOFC also allowing to mitigate

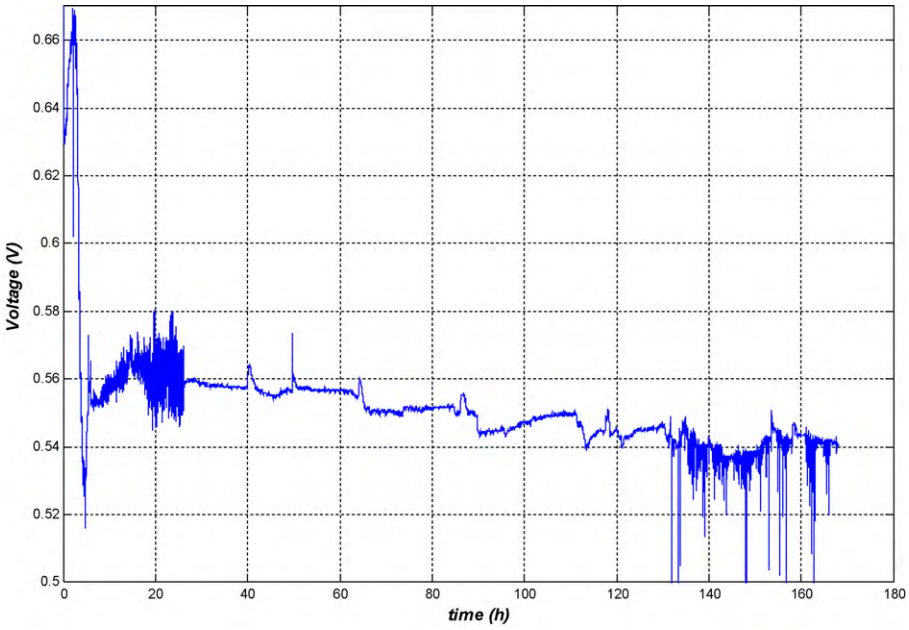

Fig. 10. Long-term experiment, 20 S cm^3 h^{-1} H_2 and 5 S cm$_3$ h^{-1} CO, S/C = 2–3 and subsequently 25 S cm^3 h^{-1} H_2, i = 0.30 A cm^{-2}.

performance degradation, as shown in Fig. 2. The test was carried on for 6 days, approximately 22 h per day. Results of this experiment are shown in Fig. 9. Here, some important conclusions can be drawn: (i) the daily cell voltage reduction was approximately 3.0%, whereas the overall decrease (6 days) is 16.1%; (ii) a significant decrease in cell voltage is achieved between day 1 and day 2 of test, whereas lower decrease is detected between day 2 and day 3 and between day 4 and 5: such variations may be due to the movements on the electrical wires and the possible changes in microstructure of the cell. The trend shown in this figure clearly validate the conclusions postulated in Fig. 2, regarding the possible sources of degradation of this kind of cell.

A second long-term test was performed in order to evaluate the resistance to carbon deposition of the micro-tubular SOFC under investigation. The test was planned to be performed for a week of continuous operation by a mixture of 20 S cm^3 h^{-1} of H_2 and 5 S cm^3 h^{-1} of CO, at 0.30 A cm^{-2} current density. Results of this test are shown in Fig. 10. The test was started with the above mentioned gas mixture, showing a voltage close to 0.67 V, then after 0.42 h of operation, the operating voltage rapidly decreased to 0.63 V. Subsequently, at 2.05 h, the voltage increased up to the initial value (0.67 V). After this maximum, the voltage rapidly decreased to 0.52 V (at 4.7 h). At this point, it was clear that carbon deposition was occurring and that this phenomena would have determined a complete cell fail in few hours. Therefore, in order to prevent this rapid failure, from this time to the end of the test, the cell was fed by 25 Scm^3 h^{-1} of humidified hydrogen, closing CO supply. This is clearly visible in Fig. 10, where cell potential is shown to re-increase up to 0.55 V. This rapid increase may be ascribed to some reduction of the magnitude of the degradation sources discussed above. However, the magnitude of voltage increase is so significant that it is reasonable to assume that this phenomenon is due to some new reactions occurring in the cell. In this study, although not evident from the experimental point of view, the authors postulated that this increase is due to the fact that, without CO, the equilibrium of reactions 9 and 10 was moved to left, allowing some of the carbon deposited to recombine with H_2O or CO_2, re-increasing cell active area [4,25,32]. Then, after approximately 21 h of unstable operation (probably due to the unstable equilibrium of reactions 9 and 10), the operating voltage approaches the stable value of 0.56 V. Subsequently, an unavoidable degradation of cell performance determines a decrease of cell voltage to 0.54 V. During the last part of the test, the operating voltage showed a significant instability, probably due to the changes in SOFC microstructure, cracks and micro-cracks formation and electrical wires detachment.

6. Conclusions

In this paper, the electrochemical performance of an anode supported micro-tubular solid oxide fuel cell fed by different fuel mixtures has been investigated. The micro-tubular SOFC used is anode supported, consisting of a NiO and $Gd_{0.2}Ce_{0.8}O_{2-x}$ (GDC) cermet anode, a thin GDC electrolyte, and a $La_{0.6}Sr_{0.4}Co_{0.2}Fe_{0.8}O_{3-y}$ (LSCF) and GDC cermet cathode. The cells were fed by hydrogen, carbon monoxide, water and methane in different combinations. During the tests, the calculated polarization curves showed a significant performance degradation both with sole hydrogen as fuel and with carbonaceous fuel mixtures. In the first case, the degradation is mainly due to cracks formation and subsequent delamination and to contact problems of the electrical wires. This latter problem is probably dominant over the other sources of degradation. In case of CO mixtures, the cell showed a slight degradation with respect to the case of H_2. Therefore, in this case the lower voltage may be ascribed mainly to the dilution in fuel flow. Conversely, in case of CH_4 mixtures, these phenomena are largely lower than carbon deposition which may block the cell electrochemistry after few hours of operations. In fact, at the considered operating temperature, CH_4 and CO are slowly consumed by the SMR and WGS reactions so that these substances are massively converted in C by the carbon deposition reactions. Results showed that the cell under investigation is dramatically sensitive to the presence of CO and CH_4 and that the ceria-based material only allow the delay the carbon deposition but are not capable to inhibit this phenomenon. Future study will include detailed tests (SEM, dilatometry, etc.) in order to accurately evaluate the exact source of this degradation. Simultaneously, additional experiments will be performed changing the SOFC materials, implementing copper-based materials, aiming at reducing this degradation.

References

[1] C.M. Dikwal, W. Bujalski, K. Kendall, Journal of Power Sources 181 (2008) 267–273.
[2] Y. Funahashi, T. Suzuki, Y. Fujishiro, M. Awano, Journal of Power Sources 163 (2007) 731–736.
[3] M.C. Williams, J.P. Strakey, W.A. Surdoval, L.C. Wilson, Solid State Ionics 177 (2006) p2039.
[4] C. Singhal, K. Kendall, High temperature Solid Oxide Fuel Cells, Elsevier, 2003.
[5] V.M. Janardhanan, O. Deutschmann, Journal of Power Sources 172 (2007) 296–307.
[6] A. Arpornwichanop, N. Chalermpancha, Y. Patcharavorachot, S. Assabumrungrat, M. Tade, International Journal of Hydrogen Energy 34 (2009) 7780–7788.
[7] A. Lanzini, P. Leone, International Journal of Hydrogen Energy 35 (2010) 2463–2476.
[8] J.M. Klein, C. Roux, Y. Bultel, S. Georges, Journal of Power Sources 193 (2009) 331–337.
[9] A. Weber, B. Sauer, B. Muller, D. Herbstritt, E. Ivers-Tiffee, Solid State Ionics 152/153 (2002) 543–550.
[10] M. Mori, Y. Hiei, N.M. Sammes, Solid State Ionics 135 (2000) 743.
[11] J. Turner, K. Rajeshwar, Electrochemical Society Interface 13-3 (2004) 24.
[12] K. Kendall, Journal of Power Sources 71 (1998) 268.
[13] X. Zhou, M. Ma, F. Deng, G. Meng, X. Liu, Journal of Power Sources 162 (2006) 179.
[14] S. Livermore, R. Ormerod, Journal of Power Sources 86 (2000) p411.
[15] U.B. Pal, S.G.W. Gong, FY 2004 Annual Report, Office of Fossil Energy Fuel Cell Program, 262, 2004.
[16] J. Pusz, A. Mohammadi, N. Sammes, ASME Journal of Fuel Cell Science and Technology 4 (3) (2006) 482–486.
[17] N.M. Sammes, Y.D.R. Bove, Journal of Power Sources 145 (2005) 228.
[18] T. Suzuki, T. Yamaguchi, Y. Fujishiro, M. Awano, Journal of Power Sources 160 (2006) 73.
[19] V. Lawlor, S. Griesser, G. Buchinger, A.G. Olabi, S. Cordiner, D. Meissner, Journal of Power Sources 193 (2009) 387–399.
[20] K. Kendall, C.M. Finnerty,.G. Saunders, J.T. Chung, Journal of Power Sources 106 (2002) 323–327.
[21] J. Pusz, A. Smimova, A. Mohammadi, N. Sammes, Journal of Power Sources 163 (2007) 900–906.
[22] A. Dihir, K. Kendall, Journal of Power Sources 181 (2008) 297–303.
[23] F. Calise, G. Restucccia, N. Sammes, Journal of Power Sources 195 (4) (2010) 1163–1170.
[24] The Open University Data book - S247 Inorganic Chemistry: Concepts and Case Studies.
[25] C.M. Finnerty, The Catalysis and Electrical Performance of Nichel-based/zirconia Fuel Reforming Anodes in Solid Oxide Fuel Cells Running on Methane, Keele University, 1998.
[26] D. Huang, K.R. Venkatachari, G.C. Stangle, Journal of Materials Research 10 (1995) 762–773.
[27] S.H. Clarke, A.L.D.K. Pointon, et al., Catalysis Today 38 (2007) 411–423.
[28] K. H. Cunningham, C.M.F.a.R.M.O., Proc. 5th Int. Symp. on SOFCs, the electrochemical Society, 1997, pp. 973–982.
[29] E. Riensche, P.C.J. Meusinger, Proc.3th European Solid Oxide Fuel Cell Forum, 1998, pp. 193–204.
[30] A. Scholten, S.T. van Schaaik, Ir. M. van Driel, Proc. 3th European Solid Oxide Fuel Cell Forum, 1998, pp. 205–216.
[31] Yamazaki, K. Tomishige, K. Fujimoto, Applied Catalysis A: General 136 (1996) 4956.
[32] G.A. Somorjai, Introduction to Surface Chemistry and Catalysis, John Wiley and Sons Inc., New York, 1994.
[33] S. Tsang, J.B. Claridge, M.L.H. Green, Catalysis Today 23 (1995) 3–15.
[34] I.V. Yentekths, Y.J.S. Neophytides, S. Bebelis, C.G. Vayen, Proc. 3rd Int. Symp. on SOFC, 1993.
[35] M.V. Twigg, Catalyst Handbook, 2th ed., Manson Publishing, 1996.
[36] C.H. Bartholomew, Catalysis Reviews-Science and Engineering 24 (1982) 68–112.
[37] D.L. Trimm, Catalysis Today 37 (1997) 233–238.
[38] R.T.K. Baker, M.S. Kim, A. Chambers, C. Park, N.M. Rodriguez, Studies in Surface Science and Catalysis 111 (1997) 99–109.
[39] J.R. Rostrup-Nielson, Symposium on the Science of Catalysis and its Application in Industry, FPDIL, 1979, p. 39.
[40] J. Zielinski, Journal of Molecular Catalysis 79 (1993) 187–198.
[41] T. Borowieckj, A. Gotebiowski, Catalysis Letters 25 (1994) 309–313.
[42] A.P.E. York, J.B. Claridge, A.J. Brungs, S.C. Tsang, M.L.H. Green, Chemical Communication (1997) 39–40.
[43] M. Mogensen, E.A. Hazbun, Proceedings of 17th Riso International Symposium, 1996, pp. 77–100.
[44] J. Misuzaki, E.A. Hazbun, Journal of Electrochemical Society 14 (1994) 2129–2134.
[45] J. Divisek, E.A. Hazbun, Journal of Power Sources 49 (1994) 257–270.
[46] R.J. Aalberg, E.A. Hazbun, Proc. 5th Int. Symp. on SOFCs, The Electrochemical Society, 1997, pp. 557–564.
[47] M. Mogensen, High Temperature Electrochemistry (1993) 117–133.
[48] V.D. Belyaev, Applied Catalysis A: General 133 (1995) 47–57.
[49] K.V. Galloway, N.M. Sammes, Journal of Electrochemical Society 156 (2009) B526–B531.